Int. J. Electrochem. Sci., 10 **(2015)** 8005 - 8016

International Journal of
ELECTROCHEMICAL
SCIENCE
www.electrochemsci.org

$Co(CO_3)_{0.5}(OH)•0.11H_2O$/Graphene Composites for Supercapacitors

Yanhua Li[1], *Jingbo Li*[1,*], *Shiying Zhang*[1], *Nanfang Wang*[2], *Zhi Zhou*[3]

[1] Hunan Province Key Laboratory of Applied Environmental Photocatalysis, Changsha University, Changsha 410022, China
[2] School of Chemistry and Chemical Engineering, Hunan Institute of Engineering, Xiangtan 411104, China
[3] College of Science, Hunan Agricultural University, Changsha 410128, China
[*]E-mail: lijinbo_yin@163.com

Received: 8 July 2015 / *Accepted:* 12 August 2015 / *Published:* 26 August 2015

$Co(CO_3)_{0.5}(OH)•0.11H_2O$/graphene composites are synthesized by a hydrothermal method through altering reaction time. Their capacitive performance is studied. The results show the that the crystallite size of $Co(CO_3)_{0.5}(OH)•0.11H_2O$ in the composites increases when reaction time prolongs. The morphology of $Co(CO_3)_{0.5}(OH)•0.11H_2O$ in the composites consists of flake and rod structures and remains unchanged when reaction time prolongs. The specific capacitance of the composites decreases when the composites prepared in long reaction time. $Co(CO_3)_{0.5}(OH)•0.11H_2O$/GNS-8 ($Co(CO_3)_{0.5}(OH)•0.11H_2O$/graphene composites prepared for 8 h) electrode possesses the largest specific capacitance. A specific capacitance of 197.4 F g^{-1} is obtained at 0.2 A g^{-1} in $Co(CO_3)_{0.5}(OH)•0.11H_2O$/GNS-8 electrode and its specific capacitance reduces to 136.2 F g^{-1} at 1.8 A g^{-1}. 69% of the specific capacitance is remained. The specific capacitance after 2400 cycles reaches 364.5 F g^{-1} at 0.2 A g^{-1}, which is 184.7% of initial specific capacitance.

Keywords: Supercapacitors, Graphene, $Co(CO_3)_{0.5}(OH)•0.11H_2O$, composites

1. INTRODUCTION

Currently, supercapacitors have attracted tremendous attention due to their high power density, long cyclic stability, and fast charge–discharge characteristics [1]. However, their energy density is inferior to that of batteries. The energy density of supercapacitors relies on operating voltage and capacitance, the values of which are determined mainly by properties of electrode materials [2]. Therefore, various electrode materials have been investigated, including carbon-based materials,

transition metal oxides, conducting polymers, and their composites. Among electrode materials, Co_3O_4 for supercapacitors exhibits environment safety, low cost, high theoretical capacitance, and favorable pseudocapacitive characteristics [3]. However, Co_3O_4 is usually synethesized with a two-step procedure [4]. Co-based intermediate compounds such as $CoCO_3$, $Co(OH)_2$, and $Co(CO_3)_{0.5}(OH)•0.11H_2O$ are first synthesized. Afterwards, Co-based intermediate compounds are calcined in air to obtain Co_3O_4. For exmaple, porous Co_3O_4 nanowires were prepared by annealing $Co(CO_3)_{0.5}(OH)•0.11H_2O$ intermediate compound synthesized via a hydrothermal method [4]. The specific capacitance of above Co_3O_4 nanowires is 248 F g^{-1} at 2 A g^{-1}. However, the capacitive characteristics of $Co(CO_3)_{0.5}(OH)•0.11H_2O$ intermediate compound has not been reported yet.

Graphene is applied as supercapacitors material due to its remarkably electron conductivity, large theoretical specific surface area, excellent mechanical strength and superior chemical stability [5-7]. Ruoff and co-workers synthesized chemically modified graphene, which showed the specific capacitances of 135 F g^{-1} in aqueous electrolytes [8]. Subsequently, they reported graphene-based supercapacitor material, which exhibited a specific capacitance of 166 F g^{-1} in ion liquid [6]. However, graphene sheets tend to form irreversible agglomerates or even restack to form graphite, which dramatically reduces specific surface area and consequently results in unsatisfactory capacitance performance [9-11]. $Co(CO_3)_{0.5}(OH)•0.11H_2O$ anchored on graphene to form $Co(CO_3)_{0.5}(OH)•0.11H_2O$/graphene composites is an effective strategy to prevent serious agglomeration or restacking of graphene nanosheets and boost the capacitive performance of graphene material.

Herein, we develop a simple one-step hydrothermal approach to synthesize $Co(CO_3)_{0.5}(OH)•0.11H_2O$/graphene composites. Meanwhile, the effect of the reaction time on the morphology and size of $Co(CO_3)_{0.5}(OH)•0.11H_2O$ in the composites is also investigated in detail. Furthermore, we present the investigation on electrochemical performance $Co(CO_3)_{0.5}(OH)•0.11H_2O$/graphene composites for supercapacitors, demonstrating advantages as electrode material for supercapacitors.

2. EXPERIMENTAL

2.1. Synthesis and characterization of $Co(CO_3)_{0.5}(OH)•0.11H_2O$/graphene composites

Graphite oxide was obtained via a modified Hummers method as described previously [9, 12]. The as-obtained graphite oxide was soaked into 0.5 mol L^{-1} tetramethylammonium hydroxide (TMAOH) solution for 7 days. Then, subjected to dialysis with deionized water until the pH equaled 7 and dried in oven.

$Co(CO_3)_{0.5}(OH)•0.11H_2O$/graphene composites were synthesized by a simple one-step hydrothermal method as follows. 80 mg TMAOH-immersed graphite oxide was dispersed in 80 mL deionized water by ultrasonication to obtain graphene oxide nanosheets. Afterwards, 3.2 mmol $Co(NO_3)_2·6H_2O$, 6.4 mmol urea and 0.64 mmol sodium citrate were dissolved into the above solution by vigorous stirring. The blended solution was then transferred into a Teflon-lined stainless steel

autoclave and hydrothermally treated at 150 ℃ for 8 h, 16 h, and 24 h, respectively. After cooled, the obtained precipitate was washed thoroughly with deionized water and ethanol for several times, and then dried in oven. $Co(CO_3)_{0.5}(OH)•0.11H_2O$/graphene composites prepared for 8 h, 16 h, and 24 h were denoted as $Co(CO_3)_{0.5}(OH)•0.11H_2O$/GNS-8, $Co(CO_3)_{0.5}(OH)•0.11H_2O$/GNS-16 and $Co(CO_3)_{0.5}(OH)•0.11H_2O$/GNS-24, respectively. The crystallographic phase of as-prepared samples was determined by X-ray diffraction (XRD, Rigaku D/max2550VB$^+$18kw with Cu Kα radiation). The morphology of as-prepared products was observed using scanning electron microscopy (FEI Nova Nano-230).

2.2. Electrochemical measurements

Cyclic voltammogram (CV), chronopotentiometry (CP), and electrochemical impedance spectroscopy (EIS) were carried out with a CHI 660D electrochemical workstation. A three-electrode cell was adopted in electrochemical measurements. The working electrode was prepared as follows. 80 wt % of $Co(CO_3)_{0.5}(OH)•0.11H_2O$/graphene composites, 15 wt % of acetylene black, and 5 wt % of poly(tetrafluoroethylene) (PTFE) were mixed to form a slurry, and then pressed obtained-slurry on a nickel foam substrate. Finally, the working electrode dried at 110 °C for 12 h under vacuum. A platinum plate and a saturated calomel electrode (SCE) were used as the counter and reference electrodes, respectively. The electrolyte is 2 M KOH solution. EIS measurements were carried out in the frequency range from 0.01 to 10^5 Hz.

3. RESULTS AND DISCUSSION

3.1. XRD analysis

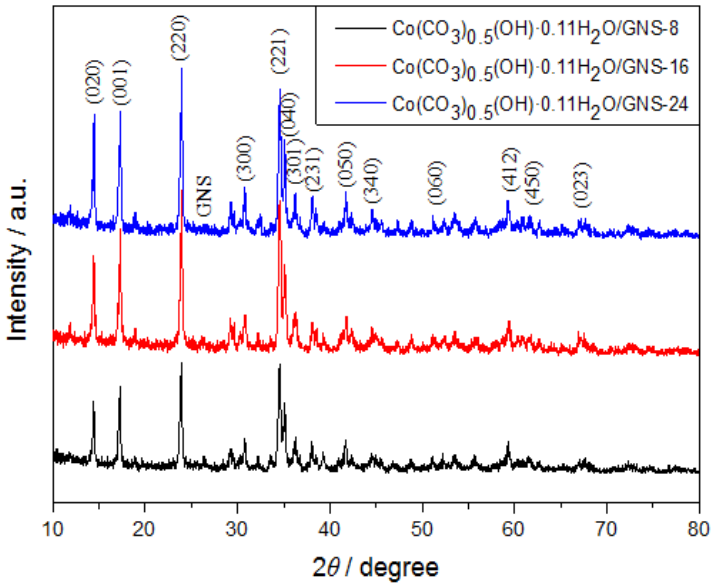

Figure 1. XRD patterns of $Co(CO_3)_{0.5}(OH)•0.11H_2O$/GNS-8 (a), $Co(CO_3)_{0.5}(OH)•0.11H_2O$/GNS-16 (b) and $Co(CO_3)_{0.5}(OH)•0.11H_2O$/GNS-24 (c).

Fig.1 displays XRD patterns XRD patterns of $Co(CO_3)_{0.5}(OH)•0.11H_2O$/GNS-8, $Co(CO_3)_{0.5}(OH)•0.11H_2O$/GNS-16 and $Co(CO_3)_{0.5}(OH)•0.11H_2O$/GNS-24. As observed in Fig.1, the XRD peaks of all the samples are attributed to orthorhombic $Co(CO_3)_{0.5}(OH)•0.11H_2O$ (JCPDS card No. 048-0083; a_0=8.792 Å, b_0=10.150 Å, c_0=4.433 Å) [4, 13, 14]. The additional peak at 2θ=26.5° are indexed to the (002) plane of graphene [15]. The formation of $Co(CO_3)_{0.5}(OH)•0.11H_2O$ in the composites can be described as following reactions [13].

$$CO(NH_2)_2+3H_2O \rightarrow 2NH_4^+ +CO_2+2OH^- \quad (1)$$

$$CO_2+2OH^- \rightarrow CO_3^{2-}+H_2O \quad (2)$$

$$Co^{2+}+0.5CO_3^{2-}+OH^-+0.11H_2O \rightarrow Co(CO_3)_{0.5}(OH)\square 0.11H_2O \quad (3)$$

The intensity of XRD peaks of $Co(CO_3)_{0.5}(OH)•0.11H_2O$ in the composites becomes stronger with increasing reaction time, which indicates that the crystallite size of $Co(CO_3)_{0.5}(OH)•0.11H_2O$ in the composites becomes larger with increasing reaction time. In other words, the crystallite size of $Co(CO_3)_{0.5}(OH)•0.11H_2O$ in the composites prepared in different reaction time from small to large follows the order of 8 h, 16 h, and 24 h.

3.2. Morphology

SEM of $Co(CO_3)_{0.5}(OH)•0.11H_2O$/GNS-8, $Co(CO_3)_{0.5}(OH)•0.11H_2O$/GNS-16 and $Co(CO_3)_{0.5}(OH)•0.11H_2O$/GNS-16 are shown in Fig. 2.

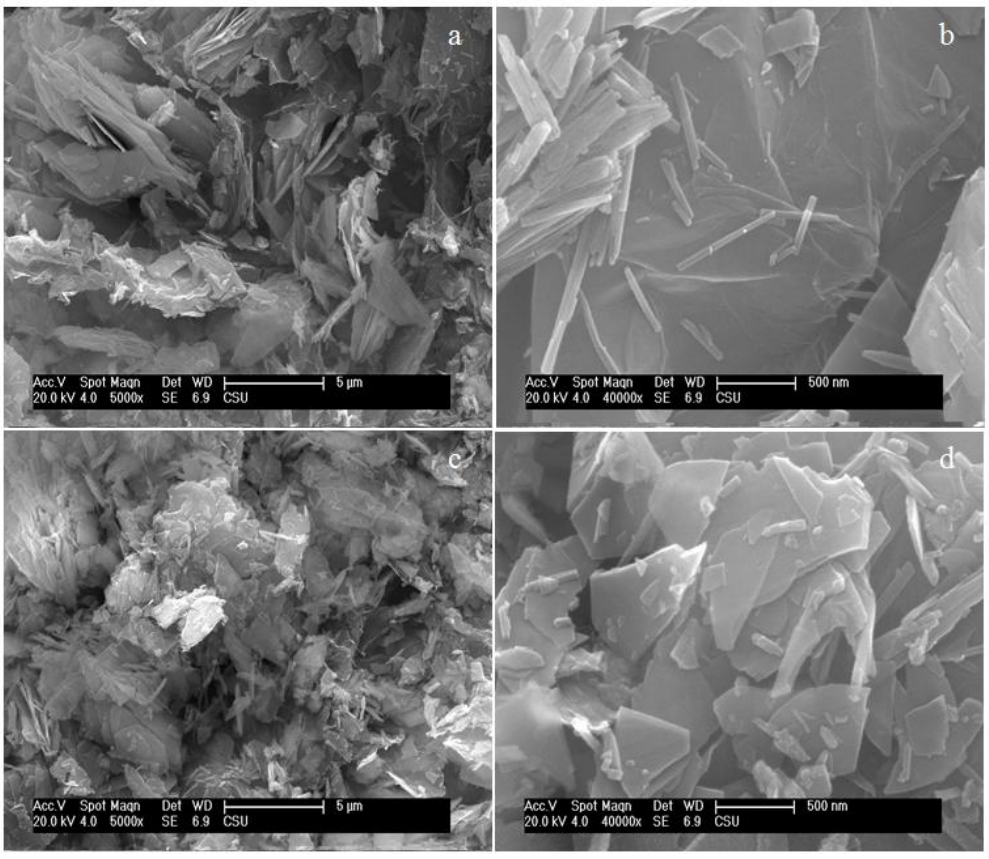

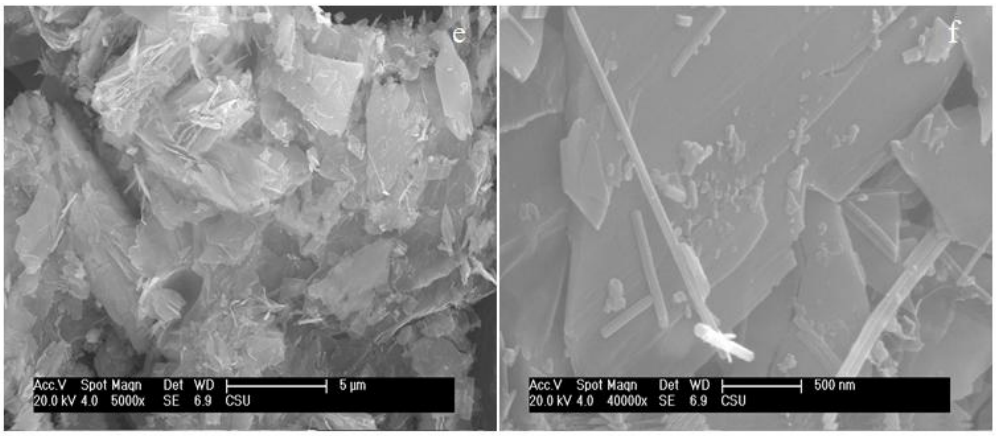

Figure 2. SEM of $Co(CO_3)_{0.5}(OH)•0.11H_2O$/GNS-8 (a, b), $Co(CO_3)_{0.5}(OH)•0.11H_2O$/GNS-16 (c, d) and $Co(CO_3)_{0.5}(OH)•0.11H_2O$/GNS-16 (e, f).

Silk-like crumpled structure is graphene and a coexistence of both nanoflake and nanorod structure is $Co(CO_3)_{0.5}(OH)•0.11H_2O$. The morphology of $Co(CO_3)_{0.5}(OH)•0.11H_2O$ in the composites has little change with the increase of reaction time from 8 h to 24 h, indicating that the morphology $Co(CO_3)_{0.5}(OH)•0.11H_2O$ in the composites hardly depends on the reaction time.

3.3. Electrochemical capacitor property

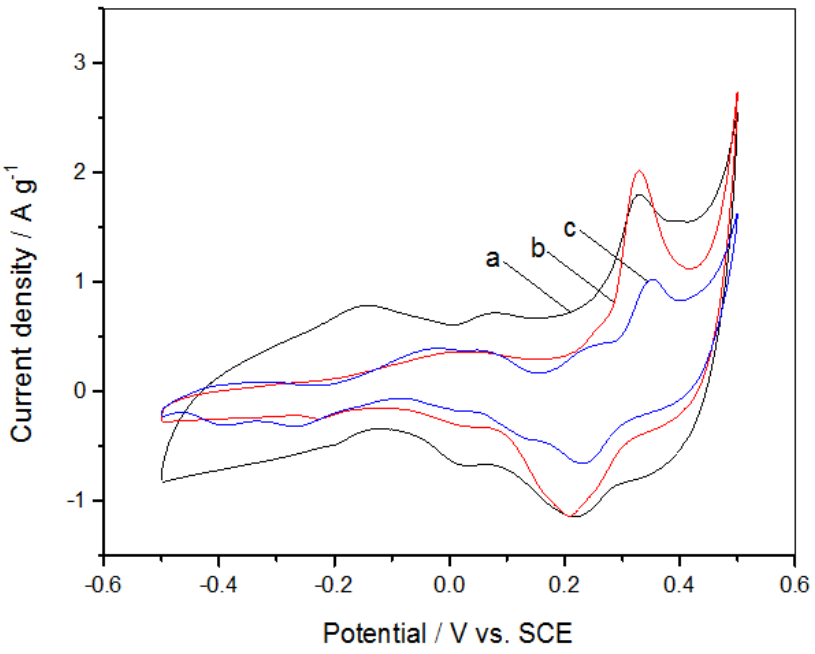

Figure 3. Cyclic voltammograms of $Co(CO_3)_{0.5}(OH)•0.11H_2O$/GNS-8 electrode (a), $Co(CO_3)_{0.5}(OH)•0.11H_2O$/GNS-16 electrode (b) and $Co(CO_3)_{0.5}(OH)•0.11H_2O$/GNS-24 electrode (c) within a potential range from -0.1 to 0.5 V in a 2 M KOH solution at a scan rate of 5 mV s^{-1}.

$Co(CO_3)_{0.5}(OH)•0.11H_2O$/GNS-8 electrode, $Co(CO_3)_{0.5}(OH)•0.11H_2O$/GNS-16 electrode and $Co(CO_3)_{0.5}(OH)•0.11H_2O$/GNS-24 electrode are depicted in Fig. 3. The shape of CV curves indicates that capacitance of the electrode mainly originates from pseudocapacitance [16]. Two pairs redox peaks observed in the potential range correspond to the electrode reaction as follows.

$$2Co(CO_3)_{0.5}(OH) + OH^- \leftrightarrow CoOOH + CoCO_3 + H_2O + e^- \quad (4)$$

$$CoOOH + OH^- \leftrightarrow CoO_2 + H_2O + e^- \quad (5)$$

Three electrodes show different current densities and CV area, which indicates that they possesses different specific capacitance. Among three electrodes, the current density of $Co(CO_3)_{0.5}(OH)•0.11H_2O$/GNS-8 electrode is the highest, the second is $Co(CO_3)_{0.5}(OH)•0.11H_2O$/GNS-16 electrode, and $Co(CO_3)_{0.5}(OH)•0.11H_2O$/GNS-24 electrode is the lowest. The explanation for above results is as follows. Although the morphology of $Co(CO_3)_{0.5}(OH)•0.11H_2O$ in the composites has little change, theirs crystallite size calculated from XRD in Fig. 1 ranks from small to large in this order: the composites prepared for 8 h, 16 h, and 24 h.

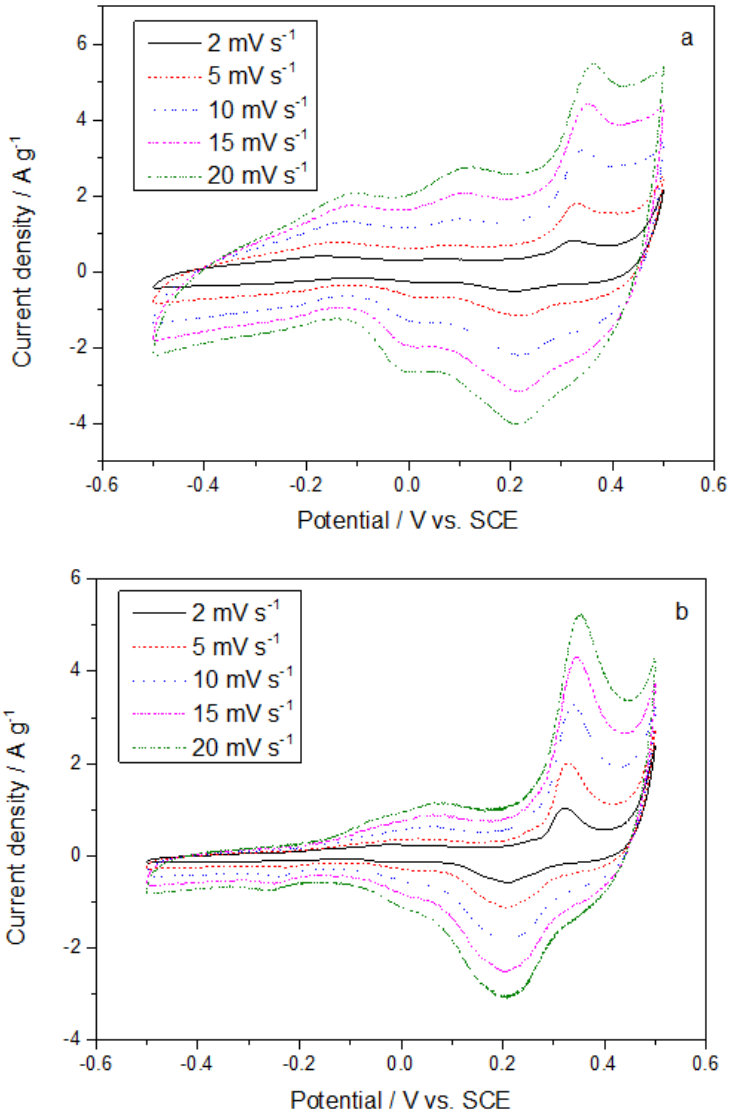

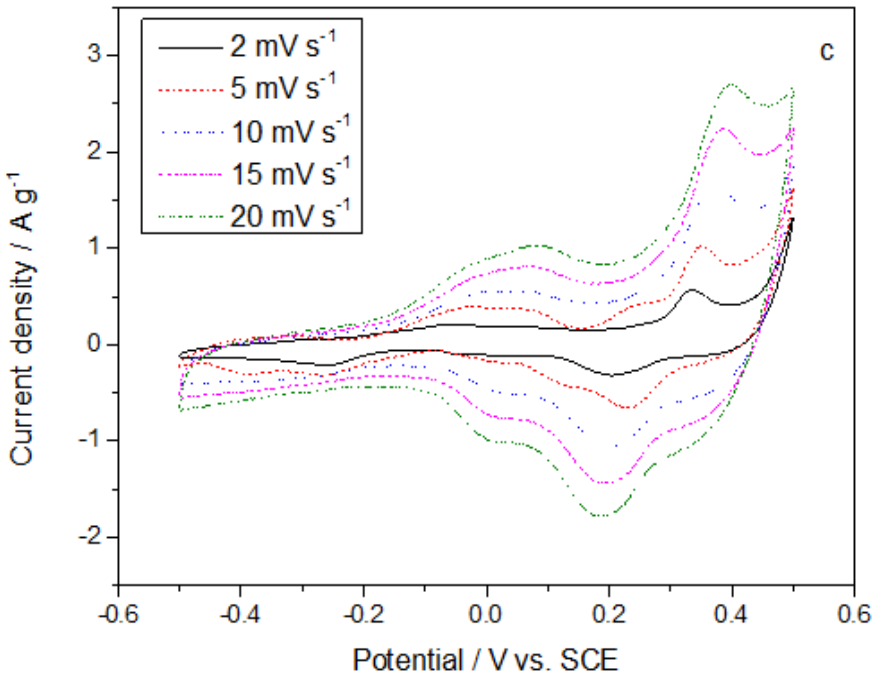

Figure 4. Cyclic voltammograms of $Co(CO_3)_{0.5}(OH)•0.11H_2O$/GNS-8 electrode (a), $Co(CO_3)_{0.5}(OH)•0.11H_2O$/GNS-16 electrode (b) and $Co(CO_3)_{0.5}(OH)•0.11H_2O$/GNS-24 electrode (c) in a 2 M KOH solution at different scan rates.

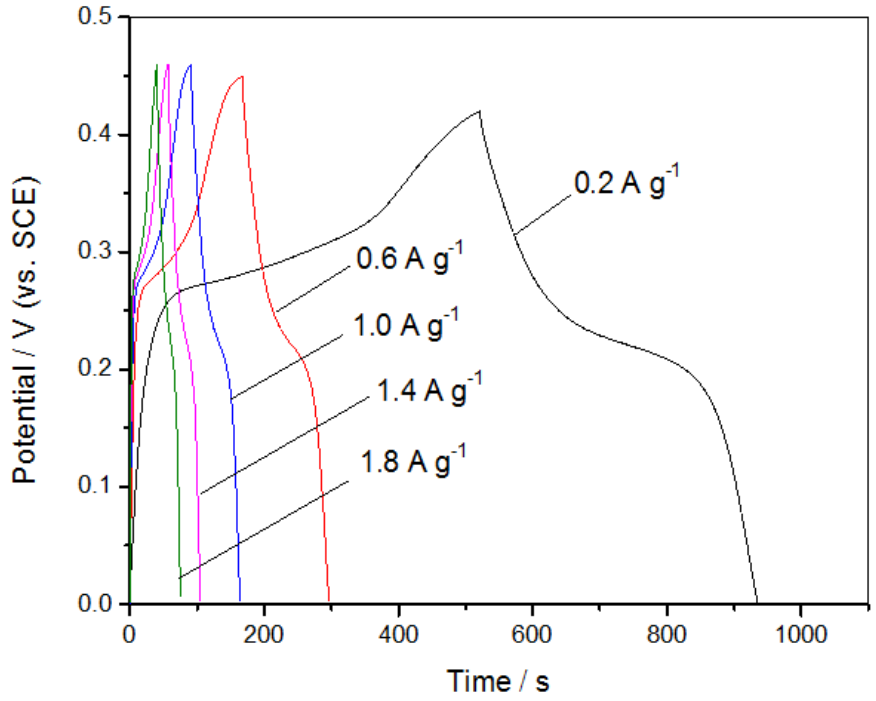

Figure 5. Galvanostatic charge–discharge curves of $Co(CO_3)_{0.5}(OH)•0.11H_2O$/GNS-8 electrode in a 2 M KOH solution at different current densities.

Fig. 4 presents cyclic voltammograms of $Co(CO_3)_{0.5}(OH)•0.11H_2O$/GNS-8 electrode, $Co(CO_3)_{0.5}(OH)•0.11H_2O$/GNS-16 electrode and $Co(CO_3)_{0.5}(OH)•0.11H_2O$/GNS-24 electrode at scan rates of 2, 5, 10, 15 and 20 mV s^{-1}. The peak current density increases when the scan rate changes from

2 to 5mV s^{-1}. In addition, the anodic peak potential shifts to high value and that of the cathodic shifts to low value when increasing the scan rate, due to the limited diffusion time [17]. The potential difference between the anodic and cathodic peak increases with increasing the scan rate due to the polarization of electrode. The anodic and cathodic current densities are in proportion to the square root of the scan rate. Similar phenomena have also been reported in the literatures [18, 19]. Fig. 4 further demostrates that the current density of three composites prepared in different reaction time from high to low ranks in this order: 8 h, 16 h, and 24 h. $Co(CO_3)_{0.5}(OH)•0.11H_2O$/graphene composites prepared for 8 h shows the highest current density, implying that it possesses the highest specific capacitance. Based on above reasons, capacitive properties of $Co(CO_3)_{0.5}(OH)•0.11H_2O$/graphene composites prepared for 8 h is studied in the present paper.

Fig. 5 shows galvanostatic charge–discharge curves of $Co(CO_3)_{0.5}(OH)•0.11H_2O$/GNS-8 electrode at different current densities. A non-linear variation in the charge process and the discharge process further verifies that capacitance performance arises from pseudo-capacitance, which matches well with the results of CV curves in Fig. 3. The specific capacitance can be calculated as follows [18, 20-22].

$$C_{sp} = \frac{It}{Vm} \tag{6}$$

where C_{sp} is the specific capacitance (F g^{-1}), I is the discharge current (A), t is the discharge time (s), V is the discharge potential window, m is the mass of active material, respectively.

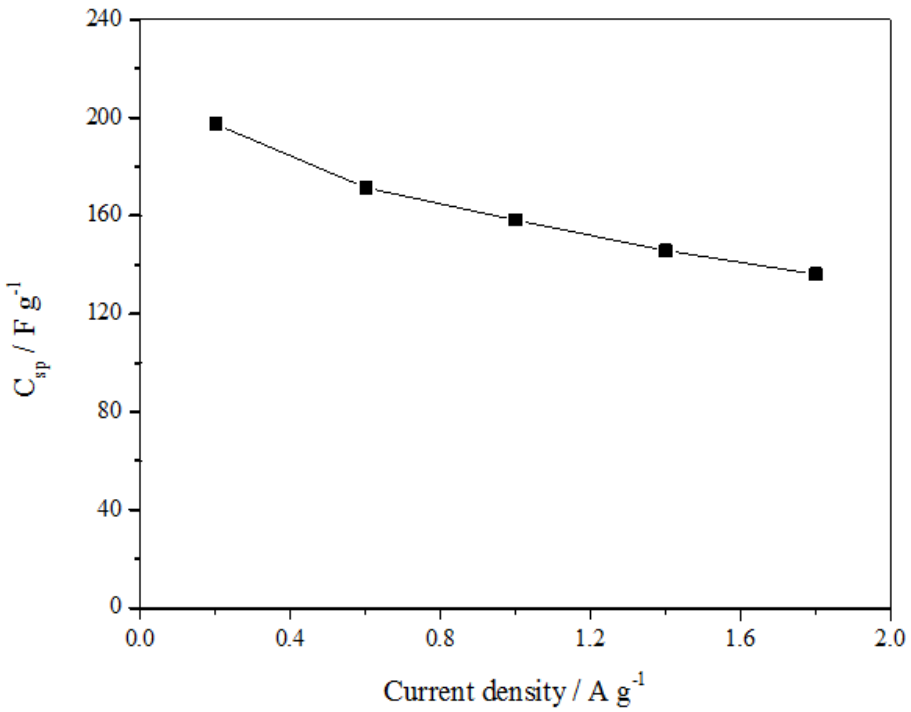

Figure 6. Relationship between the specific capacitance and the current density of $Co(CO_3)_{0.5}(OH)•0.11H_2O$/GNS-8 electrode.

Fig. 6 displays the corresponding specific capacitance of $Co(CO_3)_{0.5}(OH)•0.11H_2O$/GNS-8 electrode at the current densities of 0.2, 0.6, 1.0, 1.4 and 1.8 A g^{-1}. $Co(CO_3)_{0.5}(OH)•0.11H_2O$/GNS-8

electrode delivers a capacitance of 197.4 F g^{-1} at 0.2 A g^{-1}, which is higher than those of Co_3O_4/reduced graphene oxide [23]. Compared with that of Co_3O_4/graphene composite electrode [24], the specific capacitance of $Co(CO_3)_{0.5}(OH)•0.11H_2O$/GNS-8 electrode is slight lower. However, KOH solution as the electrolyte in the literature [24] is higher than that in the work. The electrode in KOH solution with high concentration possesses high specific capacitance [25]. Meanwhile, the specific capacitance of Co_3O_4/graphene composite in the literature [24] is calculated in the potential range from 0 to 0.4 V, which is lower than that in this work (0-0.42 V, 0-0.45 V or 0-0.46 V). The higher the potential range, the higher the energy density and the power density. Although a specific capacitance of 197.4 F g^{-1} in the work is not the highest when compared with those reported Co_3O_4/graphene or Co_3O_4/reduced graphene oxide electrodes [9, 26, 27], $Co(CO_3)_{0.5}(OH)•0.11H_2O$/graphene composites in this work were synthesized with a one-step process, which distinguishes from the two-step process [9, 27]. Moreover, the influence of the reaction time on the morphology and size of $Co(CO_3)_{0.5}(OH)•0.11H_2O$ in the $Co(CO_3)_{0.5}(OH)•0.11H_2O$/graphene composites is also investigated. The specific capacitance is 136.2 F g^{-1} at 1.8 A g^{-1}. 69% of the specific capacitance is remained.

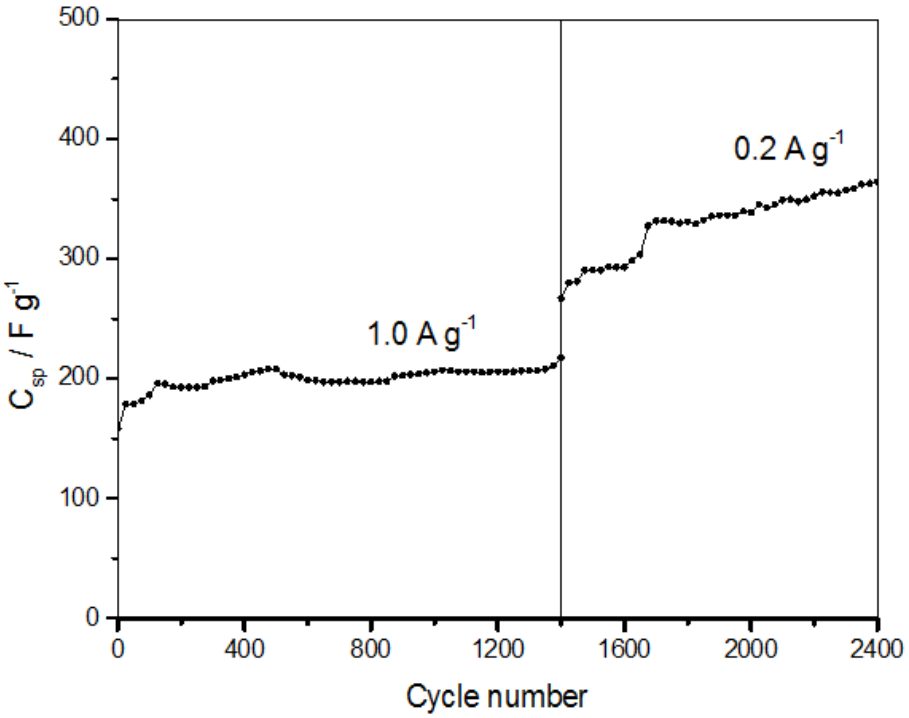

Figure 7. The cycling performance of $Co(CO_3)_{0.5}(OH)•0.11H_2O$/GNS-8 electrode.

Fig. 7 shows the cycling performance of $Co(CO_3)_{0.5}(OH)•0.11H_2O$/GNS-8 electrode. As shown in Fig. 7, $Co(CO_3)_{0.5}(OH)•0.11H_2O$/GNS-8 electrode exhibits noticeable cycling stability. The specific capacitance increases from 158.3 to 217.5 F g^{-1} when the cycle number increases from 1 to 1400 at 1.0 A g^{-1}. The specific capacitance increases from 267.2 to 364.5 F g^{-1} when the cycle number increases from 1400 to 2400 at 0.2 A g^{-1}. The specific capacitance after 2400 cycles reaches 364.5 F g^{-1} at 0.2 A g^{-1}, which is 184.7% of initial specific capacitance (A initial specific capacitance of 197.4 F g^{-1} is obtained at 0.2 A g^{-1}). The specific capacitance increases with the cycle number, instead of decreasing.

This is different from most cycling stability tests in the literatures. This is attributed to improve the surface wetting of the electrode caused by the cycle, resulting in more electroactive surface areas [9, 28]. Similar phenomena have also been reported in the literatures [17]. We previously demonstrated that the specific capacitance of Co_3O_4/graphene composites after 1000 cycles decreases in some degree [29]. Therefore, $Co(CO_3)_{0.5}(OH)•0.11H_2O$/GNS-8 exhibits excellent cycling stability when compared with Co_3O_4/graphene composites reported in our groups [9, 29].

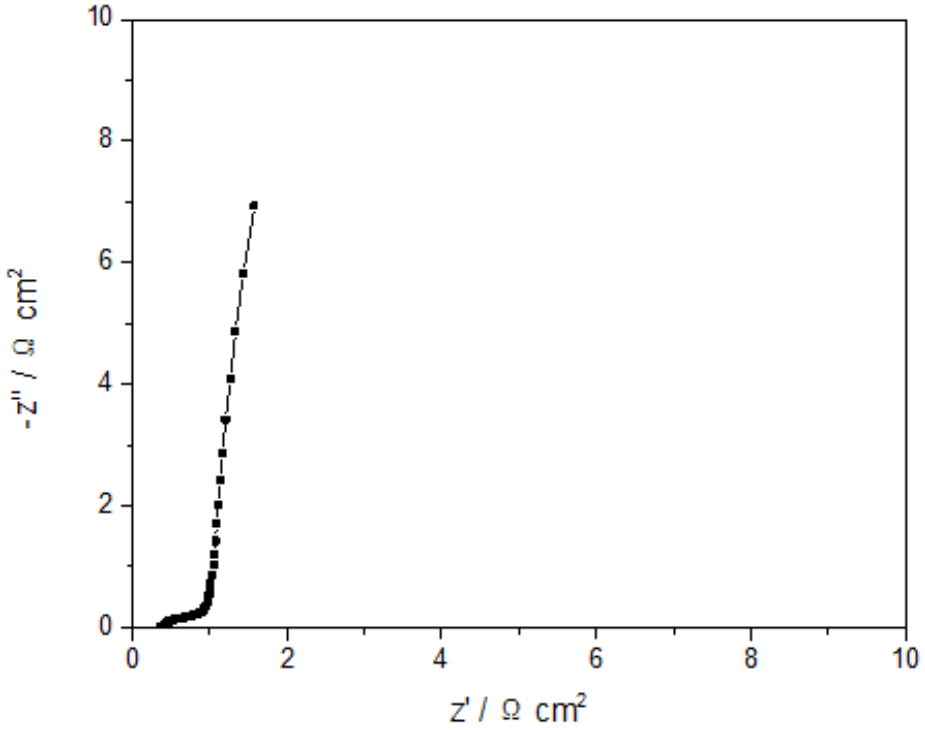

Figure 8. Nyquist plots of $Co(CO_3)_{0.5}(OH)•0.11H_2O$/GNS-8 electrode measured in a 2 M KOH solution at 0.1 V.

Fig. 8 shows Nyquist plots of $Co(CO_3)_{0.5}(OH)•0.11H_2O$/GNS-8 electrode measured at 0.1 V. Nyquist plots consists of a depressed semicircle component and a straight line component in the low frequency range. The crossover point of Nyquist plot at z' axis in the high frequency range is a combinational resistance of the electrolyte resistance, the active material intrinsic resistance, and contact resistance at the active material/the current collector interface [19, 30]. This value is 0.37 Ω cm^2, which is low because $Co(CO_3)_{0.5}(OH)•0.11H_2O$/GNS-8 electrode contains graphene with excellent electron conductivity. In the high frequency range, a depressed semicircle arises from a parallel combination of the charge-transfer resistance and the double-layer capacitance [7, 31, 32]. The straight line of the low frequency range leans more towards z" axis, indicating a good capacitive behavior in $Co(CO_3)_{0.5}(OH)•0.11H_2O$/GNS-8 electrode [32, 33].

4. CONCLUSIONS

$Co(CO_3)_{0.5}(OH)•0.11H_2O$/graphene composites are prepared by a simple one-step hydrothermal method through altering reaction time. The crystallite size of $Co(CO_3)_{0.5}(OH)•0.11H_2O$ in the composites becomes larger and its morphology almost unchanged when reaction time increases. The specific capacitance of the composites decreases when the composites prepared in long reaction time. Among three $Co(CO_3)_{0.5}(OH)•0.11H_2O$/graphene composites electrodes, $Co(CO_3)_{0.5}(OH)•0.11H_2O$/GNS-8 electrode shows the largest specific capacitance. A specific capacitance of 197.4 F g^{-1} is obtained at 0.2 A g^{-1} in $Co(CO_3)_{0.5}(OH)•0.11H_2O$/GNS-8 electrode. Its specific capacitance reduces to 136.2 F g^{-1} at 1.8 A g^{-1}. 69% of the specific capacitance is remained. The specific capacitance after 2400 cycles reaches 364.5 F g^{-1} at 0.2 A g^{-1}, which is 184.7% of initial specific capacitance, demonstrates the great advantages of $Co(CO_3)_{0.5}(OH)•0.11H_2O$/GNS-8 as supercapacitors electrode.

ACKNOWLEDGEMENTS
This work was financially supported by Science and Technology Plan Fund of Hunan Province (No. 2013GK3072), Scientific Research Fund of Hunan Provincial Education Department (No. 14B022) and Aid Program for Science and Technology Innovative Research Team in Higher Educational Institutions of Hunan Province.

References

1. S.M. Chen, R. Ramachandran, V. Mani and R. Saraswathi, *Int. J. Electrochem. Sci.*, 9 (2014) 4072.
2. Q.F. Zhang, C.M. Xu and B.G. Lu, *Electrochim. Acta*, 132 (2014) 180.
3. R.B. Rakhi, W. Chen, D.Y. Cha and H.N. Alshareef, *Nano Lett.*, 12 (2012) 2559.
4. B. Wang, T. Zhu, H.B. Wu, R. Xu, J.S. Chen and X.W. Lou, *Nanoscale*, 4 (2012) 2145.
5. M.F. El-Kady, V. Strong, S. Dubin and R.B. Kaner, *Science*, 335 (2012) 1326.
6. Y.W. Zhu, S. Murali, M.D. Stoller, K.J. Ganesh, W.W. Cai, P.J. Ferreira, A. Pirkle, R.M. Wallace, K.A. Cychosz, M. Thommes, D. Su, E.A. Stach and R.S. Ruoff, *Science*, 332 (2011) 1537.
7. Q. Guan, J.L. Cheng, B. Wang, W. Ni, G.F. Gu, X.D. Li, L. Huang, G.C. Yang and F.D. Nie, *ACS Appl. Mater. Interfaces*, 6 (2014) 7626.
8. M.D. Stoller, S.J. Park, Y.W. Zhu, J.H. An and R.S. Ruoff, *Nano Lett.*, 8 (2008) 3498.
9. X.W. Wang, S.Q. Liu, H.Y. Wang, F.Y. Tu, D. Fang and Y.H. Li, *J. Solid State Electrochem.*, 16 (2012) 3593.
10. H.W. Wang, H. Yi, X. Chen and X.F. Wang, *J. Mater. Chem. A*, 2 (2014) 1165.
11. X. Zhang, H. Zhang, C. Li, K. Wang, X. Sun and Y. Ma, *RSC Adv.*, 4 (2014) 45862.
12. W.S. Hummers and R.E. Offeman, *J. Am. Chem. Soc.*, 80 (1958) 1339.
13. S.L. Xiong, J.S. Chen, X.W. Lou and H.C. Zeng, *Adv. Funct. Mater.*, 22 (2012) 861.
14. Y. Wang, Z.Y. Zhong, Y. Chen, C.T. Ng and J.Y. Lin, *Nano Research* 4(2011) 695.
15. S.B. Yang, G.L. Cui, S.P. Pang, Q. Cao, U. Kolb, X.L. Feng, J. Maier and K. Mullen, *ChemSusChem*, 3 (2010) 236.
16. M.S. Wu, C.Y. Huang and K.H. Lin, *J. Power Sources*, 186 (2009) 557.
17. B.R. Duan and Q. Cao, *Electrochim. Acta*, 64 (2012) 154.
18. Y.H. Li, K.L. Huang, S.Q. Liu, Z.F. Yao and S.X. Zhuang, *J. Solid State Electrochem.*, 15 (2011) 587.
19. F.L. Luo, J. Li, Y. Lei, W. Yang, H.Y. Yuan and D. Xiao, *Electrochim. Acta*, 135 (2014) 495.

20. Y.H. Li, K.L. Huang, D.M. Zeng, S.Q. Liu and Z.F. Yao, *J. Solid State Electrochem.*, 14 (2010) 1205.
21. X. Yu, B. Lu and Z. Xu, *Adv. Mater.*, 26 (2014) 1044.
22. Y.H. Li and Q.Y. Chen, *Asian J. Chem.*, 24 (2012) 4736.
23. W.W. Zhou, J.P. Liu, T. Chen, K.S. Tan, X.T. Jia, Z.Q. Luo, C.X. Cong, H.P. Yang, C.M. Li and T. Yu, *Phys. Chem. Chem. Phys.*, 13 (2011) 14462.
24. J. Yan, T. Wei, W. Qiao, B. Shao, Q. Zhao, L. Zhang and Z. Fan, *Electrochim. Acta*, 55 (2010) 6973.
25. Y.Y. Gao, S.L. Chen, D.X. Cao, G.L. Wang and J.L. Yin, *J. Power Sources*, 195 (2010) 1757.
26. G.Y. He, J.H. Li, H.Q. Chen, J. Shi, X.Q. Sun, S. Chen and X. Wang, *Mater. Lett.*, 82 (2012) 61.
27. B. Wang, Y. Wang, J. Park, H. Ahn and G.X. Wang, *J. Alloys Compd.*, 509 (2011) 7778.
28. Y.R. Zhu, X.B. Ji, Z.P. Wu, W.X. Song, H.S. Hou, Z.B. Wu, X. He, Q.Y. Chen and C.E. Banks, *J. Power Sources*, 267 (2014) 888.
29. Y.H. Li, S.Y. Zhang, Q.Y. Chen and J.B. Jiang, *Int. J. Electrochem. Sci.*, 10 (2015) 6199.
30. W.L. Yang, Z. Gao, J. Ma, J. Wang, B. Wang and L.H. Liu, *Electrochim. Acta*, 112 (2013) 378.
31. M.S. Wu and H.H. Hsieh, *Electrochim. Acta*, 53 (2008) 3427.
32. Y.H. Li, K.L. Huang, Z.F. Yao, S.Q. Liu and X.X. Qing, *Electrochim. Acta*, 56 (2011) 2140.
33. H.F. An, Y. Wang, X.Y. Wang, N. Li and L.P. Zheng, *J. Solid State Electrochem.*, 14 (2010) 651.